ABSTRACT

HU, YUHAN. Human-Machine Interaction System Reliability Model and Its Application with Multiple Dependent Degradation Processes and Random Shocks. (Under the direction of Dr. Mengmeng Zhu).

Reliability models have been widely applied in different critical applications. Many studies have shown that human factors greatly affect the performance of the machine. However, most system reliability models neglect the impact of human behaviors on the performance of the machine. We thus propose a new human-machine interaction (HMI) system reliability model, in which the health state of the machine is not only affected by internal and external factors but also human behaviors. The human behaviors in this thesis are illustrated by human situation awareness (HSA). HSA can be influenced by many factors, such as time, automation level, attention, and workload. Here, time and automation levels are chosen to model HSA. The proposed HMI system reliability model considers not only the impact of HSA on the health state of the machine but also random shocks caused by disruptive events and inherent multiple degradation processes of the machine. The impacts of HSA and random shocks will be reflected on the system as incremental change and sudden jump on degradation rate. Multiple degradation processes are dependent in this study. Copula method is thus applied to model such dependent relationships. The proposed model is firstly demonstrated by a simulated case, then by the real-world data collected from a battery management system in electric vehicles (EVs). Sensitivity analysis is further conducted in these two examples to analyze the impacts of parameters on system reliability prediction. The comparisons of system reliability prediction with different copulas are illustrated in these two examples.

Human-Machine Interaction System Reliability Model and Its Application with Multiple Dependent Degradation Processes and Random Shocks

by
Yuhan Hu

A thesis submitted to the Graduate Faculty of
North Carolina State University
in partial fulfillment of the
requirements for the degree of
Master of Science

Textile Engineering

Raleigh, North Carolina
2021

APPROVED BY:

Dr. Mengmeng Zhu Committee Chair	Dr. A. Blanton Godfrey
Dr. Xiangwu Zhang	Dr. Wenbin Lu

DEDICATION

I dedicated this work to my family. I could not finish this without their support.

BIOGRAPHY

Yuhan Hu received the B.S. degree in fashion design and engineering from Zhejiang Sci-Tech University, Hangzhou, Zhejiang, China, in 2020. She is currently pursuing an M.S. degree in textile engineering at NC State University, Raleigh, NC, USA. Her research interest focuses on system reliability modeling.

ACKNOWLEDGMENTS

I would like to express my special thanks to my advisor Dr. Mengmeng Zhu who is very respective, patient, and helped me a lot in my study. I have learned a lot from the courses that she taught, which gave me a general understanding of reliability modeling and let me get started to become interested in this field. I have also learned a lot throughout this thesis from her including not only professional knowledge but also logical thinking.

I would also like to thank my committee members, Dr. A. Blanton Godfrey, Dr. Xiangwu Zhang, and Dr. Wenbin Lu, for their insightful comments and questions. Also, to my senior, Rui Wang, thank him for helping me in coding.

Last but not the least, I would like to thank my parents, who always give me many encouragements and comforts. These are such important supports to me.

TABLE OF CONTENTS

LIST OF TABLES

LIST OF FIGURES

CHAPTER 1: INTRODUCTION

With the development of mass production and the increasing demand for product quality, reliability has been intensively studied in the past few decades. It is always related with failure in one system. The failure of a system has an impressive influence on the users and the entire society. For example, in 1967, the Point Pleasant Bridge collapsed before its designed life, causing dozens of person's deaths and many injuries [1]. In 2012, 2.5 million Toyota vehicles were recalled because there was a lack of checking the safety performance of window switch materials under high temperature before putting into the market [2]. This car recall was extensive and costly. Therefore, a great number of reliability models [3-16] have been developed to assess degradation based on different scenarios, for example, multiple degradation processes of a complex system. Also, random shocks are always considered in reliability models since the system failure can also be caused by unexpectedly disruptive events. For example, Wang and Coit [3] developed a system reliability model with dependent degradation processes given that the processes are governed by a multivariate normal distribution. Wang and Pham [4] proposed a relatively complete system reliability model considering the dependencies among multiple degradation processes with the inherent system degradation and random shocks. Most system reliability models refer machine as the system. Indeed, these studies [3-16] treated machine reliability as system reliability. It is commonly assumed that a system is static throughout the lifetime, which is also the underlying assumption for most system engineering techniques nowadays. The impact on the system from the interactions between human and system are neglected in many studies. However, many studies [17-20] have shown that human behaviors can greatly impact the performance of the machine. Such impact has not been incorporated into the development of the system reliability model. Thus, in this study, our focus is on the development of a new human-machine interaction (HMI) system

reliability model, in which the health state of the machine is not only affected by internal and external factors but also human behaviors.

Human behaviors can be categorized into three groups in terms of their origins, external factors, human conditions, and human habits [21]. All these can eventually impact the machine's health state. For example, as an external factor, an incoming call may distract a driver and as a consequence, make the car suffer from the sudden brake, turning, or acceleration. This will eventually speed up the wear of braking pads, tires, and engines. Besides the external influence, human conditions (e.g., fatigue and the impact of drugs) can also result in incorrect machine operation, which may further accelerate machine's degradation and shorten the designed life span. For example, a lathe machine operator may burn the tool if the operator is under the influence of fatigue and does not pay close attention to the smoke.

The examples mentioned above illustrate the impact of human behaviors can be critical to the health status of the machine. In this thesis, human situation awareness (HSA) is employed to represent human behaviors. As described in Endsley [22], HSA is expressed as *"the perception of the elements in the environment within a volume of time and space, the comprehension of their meaning, and the projection of their status in the near future"*. In other words, HSA is a decision-making process, which can predict future status based on the assessment and interpretation of the current status. Many researchers studied how HSA can be affected by external or internal factors in the area of psychology. However, in the area of reliability engineering, none of them include HSA in the consideration of developing reliability models. In this research, we thus propose an HMI system reliability model, which not only takes into account the impact of HSA on the health state of the machine, but also random shocks caused by disruptive events and inherent multiple degradation processes of the machine. Multiple degradation processes can be modeled either

dependently or independently. In this study, the dependency between degradation processes is chosen since it represents practical scenarios in real life. Later, the copula method is applied to model such dependent relationships. The impact of HSA and random shocks will be reflected on the system as incremental change and sudden jump on degradation rate.

The remainder of this thesis is organized as follows. In Chapter 2, we review literature that studied system reliability modeling, the impacts of human behaviors on the system, and the methods of quantifying HSA. In Chapter 3, we propose an HMI system reliability model in consideration of the impact of HSA on the health state of the machine, random shocks, and multiple dependent degradation processes. Then two numerical examples are taken: one is a simulated example, the other is that we use the real-world data collected from the batteries of electric vehicles (EVs) to demonstrate the effectiveness of system reliability prediction based on the proposed model. Chapter 4 concludes this research and discusses the future direction.

CHAPTER 2: LITERATURE REVIEW

Generally, researchers incorporated multiple degradation processes to model the reliability of a complex system. These processes can be modeled both dependently and independently, and each of them has its advantage. When the processes are modeled independently, it eases the complexity of modeling, which could save time on formulation and calculation. For example, Crk et al. [5] modeled degradation processes independently and predicted system reliability by directly multiplying the reliability of each degradation process. This is an efficient way to get the reliability prediction. However, this model has the drawback that it cannot always fit practical scenarios in real life since the degradation processes are often dependent on actual conditions. Therefore, the model needs to be improved and such a model can be done under the assumption that the degradation processes are dependent. For example, Wang and Coit [3] modeled the degradation processes dependently given that the processes are governed by a multivariate normal distribution. Pan et al. [7] also proposed a dependent degradation model. This model was used for bivariate dependent degradation processes, given that they followed the Wiener process. Compared with independent degradation reliability models, the difference of dependent degradation reliability models is that we need to find a method to solve the dependency among multiple degradation processes. The copula function is widely used to solve this interaction, which is a cumulative distribution function (CDF) that can link multiple marginal probabilities. For example, Pan et al. [7] utilized the copula method to solve the dependency in bivariate degradation processes and the parameters were estimated by the Bayesian Markov chain Monte Carlo method. Reference [4, 23] applied the copula method in multiple degradation processes and estimated parameters by using the Expectation-maximization (EM) algorithm and Maximum likelihood estimation (MLE), respectively.

Besides degradation, random shocks can also cause system failure. To define the failure due to random shocks, three methods are commonly employed, namely, cumulative shock models, extreme shock models, and run shock models. To be specific, in cumulative shock models, the system will not fail until the cumulative shock damage passes its critical threshold [10]. Failures in extreme shock models happen when any single random shock damage is beyond a critical threshold [11]. Mallor and Omey [12] defined that the system fails when the number of consecutive random shocks exceeds the critical threshold.

Studies discussed above mainly talked about the system reliability models with either degradation processes or random shocks individually. However, in lots of cases, degradation and random shocks can happen simultaneously. Therefore, many researchers integrate both of them into the model. For example, to make a more practical model, Li and Pham [13] considered degradation path and cumulative random shock damage in one model to solve a maintenance problem. Lin et al. [14] used the combination of degradation and random shocks to make a reliability assessment. In this model, the degradation is represented by multi-state models and the random shock is represented by physics-based models. Not limited to the direct impact on failure, random shock can also influence machine degradation rate. Such a model is proposed in Wang et al.'s paper [15]. To represent this rate, Wang and Pham [4] introduced a time-scaled factor by adding a new term into the original variable, whose idea was borrowed from accelerating life tests; Rafiee et al. [16] built a more complete model by considering the influence of multiple random shocks in the degradation rate, namely, external shock, δ - shock, m -shock, and run shock. Moreover, degradation can also influence random shock. More specifically, the occurrence of random shock is dependent on the degradation level. For example, Fan et al. [9] modeled this

dependency according to the degradation status to classify random shock into three zones, including the damage, fatal, and safety zones.

Besides machine itself, human also plays an important role in the system performance. Studies showed humans can accelerate degradation. For example, Seo et al. [18] studied the impact of distraction tasks on machine degradation during simulated driving. The result showed that distraction tasks can cause machine degradation or even damage because it makes car control more difficult. Fan et al. [19] investigated the effects of workload and fatigue on system performance. They concluded that workload could cause fatigue and further led to bad system performance. Rahman et al. [20] conducted driving experiments under three levels of complexity and found a strong linear correlation between mental workload and driving performance. Thereby, there is a need to consider both machine and human in one model, and such model is called the HMI system. However, only a few studies proposed reliability models with human factors incorporated. Jan et al. [22] proposed a system reliability model as the product of machine reliability and human reliability to show the role of humans in HMI systems and used the human error severity index to express the impacts of human errors on the system. Havlikova et al. [23] carried out a human reliability assessment to assess the impacts of human behaviors in HMI systems based on probabilistic safety analysis.

To demonstrate and quantify the impacts of human behaviors, we discuss the factors that may affect HSA and the quantification of HSA. Time is one of the most important factors. Many researchers worked on the trend between HSA and time by different methods. De et al. [27] presented a hypothetical result of HSA by using the Situation Awareness Global Assessment Technique, which needs participants to answer queries. Time is fixed to assess HSA. The results revealed a decrease in HSA as time goes. Becerra [28] evaluated how time influences HSA under

a low automation level (LAL), which is regarded as the normal state, by using SPAM. SPAM is a real-time probe technique, which does not need to fix the time during the task. It normally takes the reaction time to the queries as a standard to qualify HSA. The results of trend analysis showed that the query reaction time increases with time linearly, which indicates a negative trend between HSA and time.

The level of automation (LOA) is another important factor that influences HSA. HSA may increase when the LOA increases because the auto system can reduce human workload. HSA may also decrease with the LOA increasing because of the deduction on the ability to respond to emergencies. Therefore, due to the different impacts of LOAs on HSA, many researchers focus on how HSA changes under different LOAs. For example, Meike et al. [29] did a simulated experiment of air traffic under three different LOAs to find out the relation between HSA and LOAs. They distinguished HSA into three levels, perception, comprehension, and prediction levels, based on the theory proposed by Endsley [22]. The result showed that HSA is the highest under the lowest LOA. Adam et al. [30] did a simulation in the Carbon Air Management System microworld, where the participants can play as an operator to monitor real situations. They differentiated LOAs based on if the function of information interpretation, decision making, and action implements needs to be done by humans. Then the relation between LOAs and HSA was analyzed by using ANOVA, which is a method to analyze the variance in one sample set. Behad et al. [31] proposed a driving simulation experiment under five different automation modes. They measured HSA under each automation mode by using the Situation Awareness Rating Technique, which is an HSA measurement that needs the participants to rate from ten different perspectives. Finally, they figured out the relation between HSA and automation modes.

CHAPTER 3: RELIABILITY MODELING DEVELOPMENT

3.1 System Description

The proposed HMI system reliability model considers multiple dependent degradation processes, random shocks, and HSA. Assume that there are n degradation processes in total, which are dependent with each other. Use k to denote a degradation process. Let each degradation process, affected by HSA, has j status, for $j = 1, 2, \dots, m$. Fig. 1 describes the state transition diagram of the HMI system with random shocks. Random shocks described in Fig. 1 have impacts on any state of any degradation process and eventually fail the system. $S_k^{(j)}$ represents the j^{th} degradation status in the k^{th} degradation process.

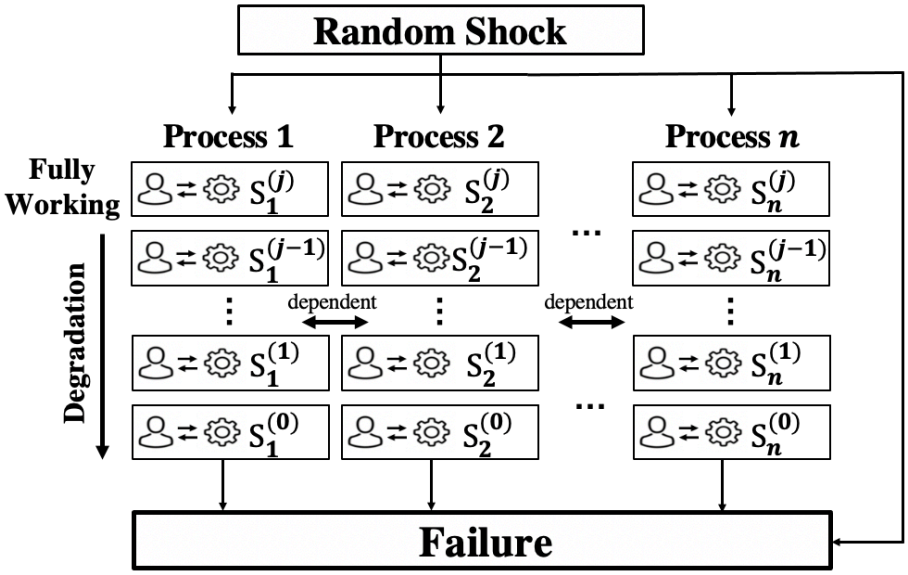

Fig. 1. State transition diagram of the HMI system subject to random shocks.

The assumptions for the proposed HMI system reliability model are given as follows.

a. In the described HMI system, every (machine) degradation process is affected by HSA.

b. All of the degradation processes are in $S_k^{(j)}$ initially and ends in $S_k^{(0)}$. It can either go to any lower status such as $S_k^{(j-1)}$, $S_k^{(j-2)}$, or go to the system failure directly.

c. Two kinds of random shocks are considered in this model [4]. Fatal random shocks will fail the HMI system immediately. Nonfatal random shocks have two types of impacts on the human-machine interaction system: incremental change and sudden jump on degradation rate.
d. HSA has two types of impacts on the system: incremental change and sudden jump on degradation rate.
e. There are multiple degradation processes in the system, which are dependent with each other. The dependency between multiple degradation processes is modeled by the copula method in this study.
f. Two situations are regarded as system failure: 1) the fatal shocks fail the system directly; 2) without fatal shocks happening, the cumulative degradation wear of any degradation process is larger than the threshold.

3.2 Human-Machine Interaction System Reliability Modeling

3.2.1 Random Shock Model

Assume that random shocks follow the homogenous Poisson process (HPP) with rate λ. This process is interpreted as a counting process, denoted as $\{N(t), t \geq 0\}$ so that the expected number of random shocks occurring per unit time $E\big(N(t)\big) = \lambda t$ [32]. In the proposed HMI system reliability model, fatal and nonfatal random shocks are considered. Assume that the average rate of fatal random shocks occurring is changed with time t, the probability of a fatal shock occurs is $p(t)$, the fatal random shock thus follows a nonhomogeneous Poisson process (NHPP) with rate $\lambda\, p(t)$. We assume that if a fatal random shock happens, the system will fail immediately; if there is no fatal shock occurred until time t, two types of impacts can be caused by nonfatal random shocks. One is sudden jumps on the degradation rate of the degradation processes. The other is

cumulative shock damage, which is represented by employing the cumulative shock model proposed by Esary et al. [10]. Let the random shocks occur at times $T_1, T_2, \dots, T_n$. The individual random shock loading is represented as $\{L_{k_1} \dots L_{k_n}\}$, following a distribution $g_k(x)$ in the k^{th} degradation process. Therefore, the cumulative nonfatal random shock, $D_k(t)$, is written as:

$$D_k(t) = \sum_{n=1}^{N1(t)} L_{k_n} \tag{1}$$

where $N_1(t)$ is the number of nonfatal random shocks.

3.2.2 Machine Degradation Wear Function

In the degradation model, additive degradation models and multiplicative degradation models are commonly used [33]. We apply the multiplicative model to describe the machine degradation wear function by using one random variable Y_k:

$$M_k(t; Y_k, \alpha_k) = Y_k \cdot \varphi_k(t; \alpha_k) \tag{2}$$

where $M_k(t; Y_k, \alpha_k)$ denotes the k^{th} machine degradation wear function, $\varphi_k(t; \alpha_k)$ represents the k^{th} mean path function with a parameter α_k. Note that $\varphi_k(t; \alpha_k)$ can be monotonically decreasing or monotonically increasing. In practice, the degradation wear of a machine usually increases because of aging, therefore, $\varphi_k(t; \alpha_k)$ is considered to be monotonically increasing in this study.

3.2.3 Human Situation Awareness Degradation Function

Two variables, time t, and automation level m are employed in the HSA function. The taxonomies of LOAs vary. In this thesis, we choose the criterion from the SAE International as the standard of LOAs, which is the most frequently cited criterion by industries since the terms utilized are commonly used and easier for customers to understand [34]. SAE International defined six levels of vehicle automation: levels 0 to 2 refer to the LAL, and levels 3 to 5 denote the high

automation level (HAL) [28]. To simplify LOAs, levels 1 and 3 will be used to denote the LAL and HAL respectively. HSA functions under the LAL and HAL were developed by conducting simulative drives. The results reported the relation between HSA and time under the LAL follows a linear distribution, which can be written as: $HSA_1 = -\partial t + \mu$, where HSA_1 is the HSA function under LAL, ∂ and μ are coefficients; HSA follows a quadratic trend under the HAL and the relation between HSA and time is written as $HSA_2 = -\sigma t^2 + \theta t + \varepsilon$, where HSA_2 is the HSA function under HAL; σ, θ, and ε are coefficients. Therefore, the HSA function is organized as:

$$HSA(t, m) = -\alpha \cdot mt^2 - \beta \cdot (-1)^m t + \gamma \cdot m + \delta \quad (3)$$

where $m = 0$ denotes LAL, $m = 1$ denotes HAL.

HSA degradation function is expressed as a multiplicative degradation model with one random variable Z_k incorporated, that is:

$$A_k(t, m; Z_k) = Z_k \cdot HSA(t, m) \quad (4)$$

where $A_k(t, m; Z_k)$ is the HSA degradation function in the k^{th} degradation process with a random variable Z_k. Since two conditions are considered in the LOA, assume that Z_k follows Bernoulli distribution in the k^{th} degradation process. Let the probability of the LAL in the k^{th} degradation process is ρ_k, the probability of the HAL is $1 - \rho_k$, $m = \{m_1, m_2\}$, $m_1 = 0$, and $m_2 = 1$, HSA degradation function can be rewritten as:

$$A_k(t, m; Z_k) = \rho_k \cdot HSA(t, m_1) + (1 - \rho_k) \cdot HSA(t, m_2) \quad (5)$$

3.2.4 Machine Degradation Function with Random shocks and Human Situation Awareness

Both random shocks and HSA can contribute to accelerating machine degradation. To solve these dependencies, we propose a new model by incorporating a time-scaled covariate factor

$F\left(t,\beta^{(k)}\right)$ into $M_k(t)$. Thus, time in the machine degradation is changed from t to $te^{F\left(t,\beta^{(k)}\right)}$. Therefore, $M_k(t)$ can be rewritten as:

$$M_k(t) = Y_k \cdot \varphi_k\left(te^{F\left(t,\beta^{(k)}\right)}; \alpha_k\right) \tag{6}$$

To quantify the impacts of random shocks and HSA on the machine degradation rate, we assume that the number of random shocks $N_1(t)$ and the total shock loadings $\sum_{n=o}^{N_1(t)} L_{k_n}$ can influence the machine degradation. For HSA, we assume the degradation of HSA with time t, denoted as $f(t)$, contributes to the machine degradation. Therefore, $F\left(t,\beta^{(k)}\right)$ is represented as:

$$F\left(t,\beta^{(k)}\right) = {\beta_1}^{(k)} N_1(t) + {\beta_2}^{(k)} \sum_{z=1}^{N1(t)} L_{k_z} + {\beta_3}^{(k)} f(t) \tag{7}$$

where ${\beta_1}^{(k)}$, ${\beta_2}^{(k)}$, and ${\beta_3}^{(k)}$ are three coefficients that should be non-negative.

The cumulative human-machine degradation wear function, $W^k(t)$, includes three terms: the machine degradation path, the incremental change in the degradation due to nonfatal random shocks, and the incremental change in the degradation because of HSA. Therefore, $W^{(k)}(t)$ can be expressed as:

$$W^{(k)}(t) = M_k(t; Y_k, \alpha_k) \; + D_k(t) + A_k(t, m; Z_k) \tag{8}$$

3.2.5 Marginal Reliability Prediction

The reliability of the k^{th} degradation process is defined as the probability that the cumulative degradation wear in the k^{th} degradation process is less than its corresponding failure threshold. The marginal reliability is expressed below:

$$\begin{aligned} R_k(t) &= P\left(W^{(k)}(t) < l^{(k)}\right) \\ &= \sum_{n=0}^{\infty} P\left(Y_k \cdot \varphi_k(te^{F\left(t,\beta^{(k)}\right)}) + D_k(t) + A_k(t) < l^{(k)} | N_1(t) = n\right) P(N_1(t) = n) \end{aligned}$$

$$= \left[P\left(Y_k \cdot \varphi_k(te^{F(t,\beta^{(k)})}) + A_k(t) < l^{(k)} | N_1(t) = 0\right) P(N_1(t) = 0) \right.$$
$$+ \sum_{\mathrm{n}=1}^{\infty} P(N_1(t) = n)$$
$$\left. \times \int_{h=0}^{l^{(k)}} P\left(Y_k \cdot \varphi_k(te^{F(t,\beta^{(k)})}) + \mathrm{h} + A_k(t) < l^{(k)} | N_1(t) = n\right) g_k^{(n)}(h)dh \right]$$

$$= \left[P\left(Y_k \cdot \varphi_k(te^{F(t,\beta^{(k)})}) + A_k(t) < l^{(k)}\right) P(N_1(t) = 0) \right.$$
$$+ \sum_{n=1}^{\infty} P(N_1(t) = n)$$
$$\left. \times \int_{h=0}^{l^{(k)}} P\left(Y_k \cdot \varphi_k(te^{F(t,\beta^{(k)})}) + \mathrm{h} + A_k(t) < l^{(k)}\right) g_k^{(n)}(h)dh \right]$$

$$= \left[exp\left(-\lambda \int_0^t q(u)du\right) F_{Y_i}\left(\frac{l^{(k)}}{\varphi_k(t)}\right) \right.$$
$$+ \sum_{n=1}^{\infty} \frac{exp\left(-\lambda \int_0^t q(u)du\right)\left(\lambda \int_0^t q(u)du\right)^n}{n!}$$
$$\left. \times \int_{h=0}^{l^{(k)}} F_{Y_k}\left(\frac{l^{(k)} - h}{\varphi_k(te^{\beta_1{}^{(k)}n + \beta_2{}^{(k)}h + \beta_3{}^{(k)}f(t)})}\right) \cdot g_k^{(n)}(h)dh \right] \quad (9)$$

where $q(u) = 1 - p(u)$, $g_k^{(n)}(h)$ is the probability density function (PDF) for cumulative nonfatal random shocks with $N_1(t) = n$ in the k^{th} degradation process.

3.2.6 System Reliability Prediction

Fatal random shocks will immediately fail the system. For each degradation process, failure occurs when the degradation wear reaches its corresponding failure threshold. The system contains n degradation processes, only if the degradation wear of each process is smaller than its critical failure threshold, the system can work. Therefore, the reliability of the system can be written as:

$$R(t) = \mathrm{P}[W^{(1)}(t) < l^{(1)}, \dots, W^{(n)}(t) < l^{(n)}]P(N_2(t) = 0) \quad (10)$$

where $W^{(i)}(t)$ denotes the degradation wear and $l^{(i)}$ is the critical threshold of the i^{th} degradation process, $N_2(t)$ is the cumulative number of fatal random shocks up to time t.

If degradation processes are independent, eq. (10) can be rewritten as:

$$R(t) = P[W^{(1)}(t) < l^{(1)}] \dots P[W^{(n)}(t) < l^{(n)}]P(N_2(t) = 0) \quad (11)$$

In this thesis, we assume that multiple degradation processes are dependent. Eq. (11) cannot be used in this case. Therefore, to address this dependency between degradation processes, the copula method is utilized to link marginal reliability functions of each degradation process. In Sklar's theorem [35], use C denotes an n-dimensional distribution function with margins F_{X_1},…, F_{X_n}. Then C is represented with n-copula C as:

$$C(X_1, X_2, \dots, X_n) = C\left(F_{X_1}(x_1), \dots, F_{X_n}(x_n)\right) \quad (12)$$

Hence, based on the definition of the copula method, the proposed HMI system reliability prediction is finalized as:

$$R(t) = C\big(R_1(t) \dots R_n(t)\big)P(N_2(t) = 0) \quad (13)$$

We assume that two degradation processes are dependent in this study, therefore, a bivariate copula is chosen. Table I lists commonly used bivariate copulas. From a mathematical perspective, copula selection can be made based on the capacity of capturing left or right tail dependence [36, 37]. For example, the Clayton copula shows the ability to capture left tail dependency, therefore, it is always chosen to fit the model in which the dependency between variables becomes obvious when they are close to negative. Gumbel copula exhibits right tail dependency, therefore, it is commonly utilized to fit the model that is more dependent between variables when they are close to infinity. The capacity of modeling positive or negative dependence is also a criterion of copula selection. Frank copula is chosen relatively often since it applies to all dependency levels between variables [38]. Most copulas can only model with positive

dependencies such as Clayton, and Gumbel copula, however, their rotated copulas may detect negative dependencies [37]. Asymmetric copulas including Clayton copula and Gumbel copula are usually used in finance to construct models with irreversible behaviors, for example, there is a sudden decrease when the trend keeps increasing [39].

TABLE I

LIST OF BIVARIATE COPULAS

Copulas	$C_\theta(u,v)$
Clayton	$(u^{-\theta}+v^{-\theta}-1)^{-\frac{1}{\theta}}$
Gumbel	$exp\left[-\left((-\log(u))^{\theta}+(-\log(v))^{\theta}\right)^{\frac{1}{\theta}}\right]$
Frank	$\left(-\frac{1}{\theta}\right)log\left[1+\frac{(\exp(-\theta u)-1)(\exp(-\theta v)-1)}{\exp(-\theta)-1}\right]$
Rotated Clayton (180°)	$((1-u)^{-\theta}+(1-v)^{-\theta}-1)^{-\frac{1}{\theta}}+u+v-1$
Rotated Gumbel (90°)	$u-exp\left[-\left((-\log(1-u))^{\theta}+(-\log(v))^{\theta}\right)^{\frac{1}{\theta}}\right]$
Rotated Frank (180°)	$(u+v-1)\left(-\frac{1}{\theta}\right)log\left[1+\frac{\left(\exp\left(-\theta(1-u)\right)-1\right)\left(\exp\left(-\theta(1-v)\right)-1\right)}{\exp(-\theta)-1}\right]$

$C_\theta(u,v)$ is the copula function, θ is the parameter, and u and v are two variables.

Take Clayton copula as an example, HMI system reliability function can be obtained as:

$$R(t)=(R_1{}^{-\theta}+R_2{}^{-\theta}-1)^{-\frac{1}{\theta}}\times\exp\left(-\lambda\int_0^t p(u)du\right) \tag{14}$$

Different copula distributions result in different system reliability functions. Regarding each situation, it is necessary to compare and select which copula distribution works better. To select the best fit copula, comparing log-likelihood, Akaike information criterion (AIC) and Bayesian information criterion (BIC) are the methods to check its goodness of fit.

Log-likelihood is the transformation of the likelihood function and maximizes the estimated parameters [40]. This is one of the methods to check the models' goodness of fit given a sample of data and unknown parameters. Higher values of log-likelihood lead to a better fit of the model. Log-likelihood function, denoted as $l(x;a)$, is written as:

$$l(x;\alpha) = \log\big(L(x;\alpha)\big) \tag{15}$$

where $L(x;\alpha) = \prod_i f(x_i;a)$ and $f(x_i;\alpha)$is PDF with unknown parameter α. Log-likelihood can be increased by adding the number of parameters. Using the value of log-likelihood as the only criteria may result in overfitting. Therefore, it is better to use different methods to check the goodness of fit besides log-likelihood. AIC and BIC are two information criteria that are widely used. The AIC and BIC value can be calculated by Eq. (16) and (17) separately [41]. Lower AIC and BIC denotes better goodness of fit. Both AIC and BIC formulas incorporate a penalty term for parameters to solve the problem of overfitting and BIC has a stronger penalty compared with AIC [42].

$$AIC = -2log\big(\hat{L}\big) + 2p \tag{16}$$

where $\hat{L}$ is the maximum likelihood estimation, p is the number of parameters.

$$BIC = -2log\big(\hat{L}\big) + plog(n) \tag{17}$$

where $\hat{L}$ is the maximum likelihood estimation, p is the number of parameters, n is the sample size.

3.2.7 Parameter Estimation

Parameters are estimated by using MLE. Based on the definition of MLE, the density function for the joint distribution is written as [4]:

$$f(x_1, \dots, x_n) = c\big(F_1(x_1), \dots, F_n(x_n)\big) \prod_{k=1}^{n} f_k(x_k) \tag{18}$$

where $c\big(F_1(x_1),\dots,F_n(x_n)\big) = C\big(F_1(x_1),\dots,F_n(x_n)\big)/\partial F_1(x_1)\dots\partial F_n(x_n)$.

The log-likelihood function with γ representing all parameters is:

$$l(\gamma) = \sum_{t=1}^{T} ln\, c\big(F_1(x_{1t}),\dots,F_n(x_{nt})\big) + \sum_{t=1}^{T}\sum_{k=1}^{n} ln\, f_k(x_{kt}) \tag{19}$$

Therefore, the MLE of γ is obtained by maximizing the function $L(\gamma)$:

$$\hat{\gamma} = \max\big(l(\gamma)\big) \tag{20}$$

3.3 Numerical Example 1

3.3.1 System Description and Marginal Reliability Prediction

Assume that the system has two degradation processes with the impact of HSA and random shocks. Let the probability of nonfatal random shock $q(t) = exp(-\sigma \cdot t)$, where $\sigma = 0.0002$. Let the random shocks occurring rate $\lambda = 0.0012$. In the first degradation process, assume that the probability of the LAL $\rho_1 = 0.5$. Y_1 in the machine degradation path function $M_k(t; Y_k, \alpha_k)$ follows Weibull distribution with CDF as $F_Y(y) = 1 - exp[-(y/\omega_1)^{\tau_1}]$ with the scale parameter $\omega_1 = 0.7$ and the shape parameter $\tau_1 = 0.5$. The random shock loadings follow a standard normal distribution with PDF as: $g_1(t) = \frac{1}{\sqrt{2\pi}} e^{-\frac{1}{2}t^2}$. HSA function $f(t)$ in the time-scaled factor is exponentially distributed with mean $\mathcal{E}_1 = 0.02$ and the coefficients in the time-scaled factor are ${\beta_1}^{(1)} = 0.04, {\beta_2}^{(1)} = 0.07, {\beta_3}^{(1)} = 0.03$. Failure threshold for the first degradation process $l_1 = 100$. Based on these parameters given above, the marginal reliability of process 1 is shown in Fig. 2. In the second degradation process, assume that the probability of the LAL is $\rho_2 = 0.5$. Y_2 follows Weibull distribution with $\omega_2 = 0.9$ and $\tau_2 = 1.2$. The random shock loadings follow an exponential distribution with mean $a = 0.0012$. HSA function $f(t)$ is exponentially distributed with mean $\mathcal{E}_2 = 0.015$. Choose the coefficients in the time-scaled factor

as ${\beta_1}^{(2)} = 0.03,\ {\beta_2}^{(2)} = 0.05,\ {\beta_3}^{(2)} = 0.02$. The failure threshold for the second degradation process is $l_2 = 200$. The marginal reliability of process 2 is shown in Fig. 3. As shown in Fig. 2 and 3, the lifetime of the first and second degradation process is around 125 and 100-time units, respectively. Besides, the reliability prediction of process 1 decreases steadily, while the reliability prediction of process 2 keeps a relatively higher level at the first 25-time units and then significantly decreases.

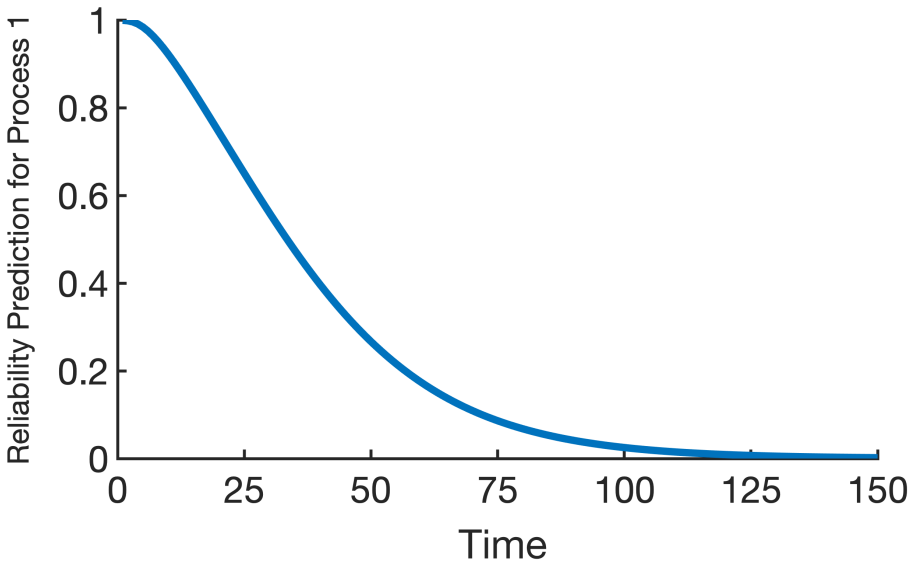

Fig. 2. Marginal reliability prediction for degradation process 1.

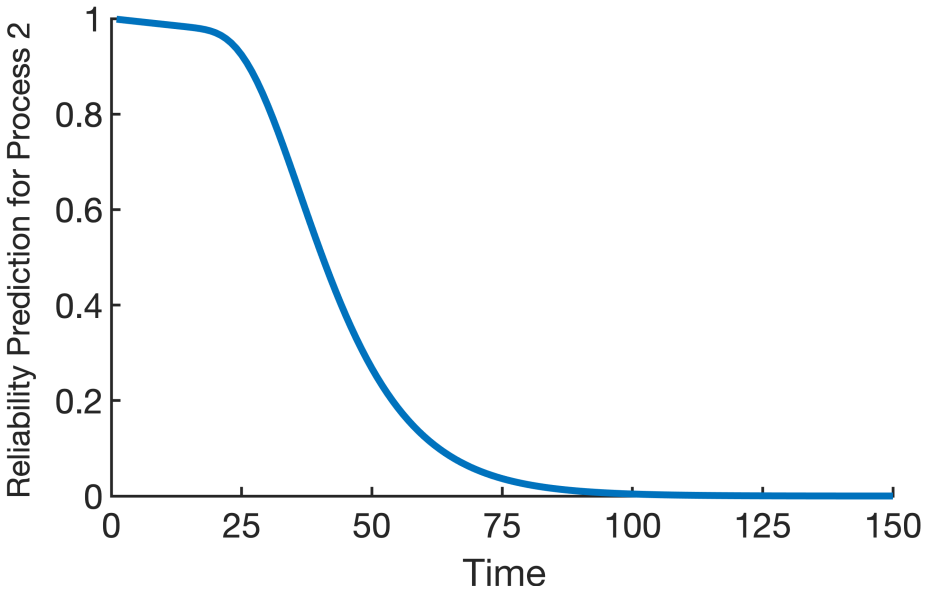

Fig. 3. Marginal reliability prediction for degradation process 2.

3.3.2 Sensitivity Analysis for Each Degradation Process

Sensitivity analysis is a commonly used method to analyze the uncertainty of outputs and validate reliability prediction models. This test can finalize how the inputs significantly influence the output variability and uncertainty [43]. In the first degradation function, we perform the sensitivity analysis for parameters ω_1, τ_1 and ρ_1, as shown in Fig. 4, 5, and 6.

According to Fig. 4, on condition that ω_1 is constant, when $\tau_1 = 0.5, 0.8, 1.2$, the corresponding lifetime to failure for process 1 is approximately 125, 100, 75-time units. In Fig. 5, when $\tau_1 = 0.5$, the lifetime to failure on the condition that $\tau_1 = 0.2, 0.7,$ and 1.2 are almost the same. In Fig. 6, we can conclude that no matter what the probability of the LAL is, the lifetime to failure does not have much difference. Besides, in Fig. 4, compared with Fig. 5 and 6, the slope of reliability prediction varies greatly and increases with the increase of τ_1. One reason that can explain this result is that the failure rate increases with time when τ is larger than 1 and decreases when τ is smaller than 1.

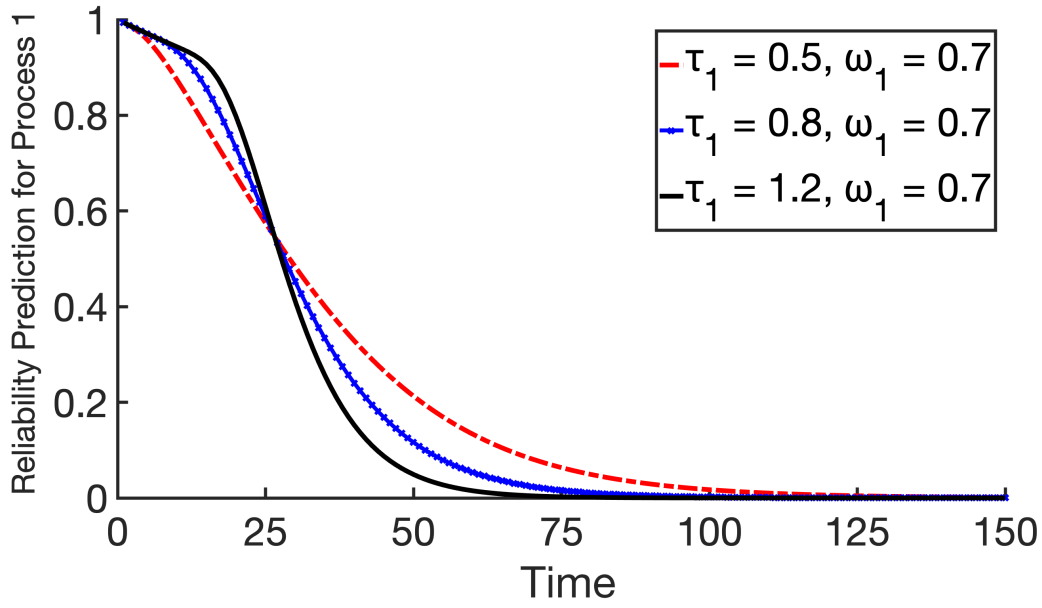

Fig. 4. Sensitivity analysis of process 1 with the changes of τ_1.

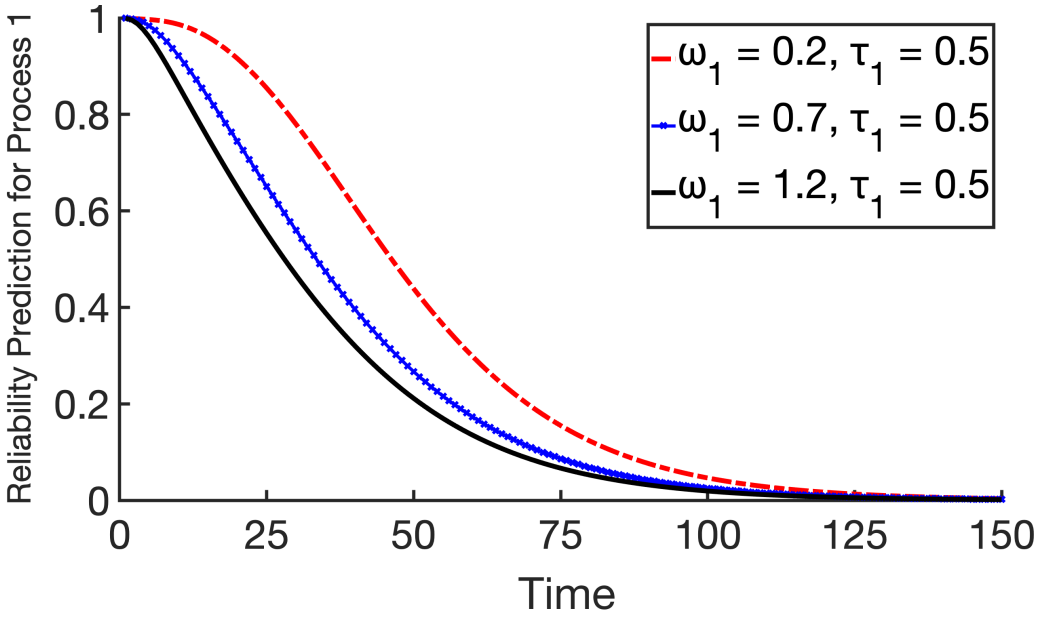

Fig. 5. Sensitivity analysis of process 1with the changes of ω_1.

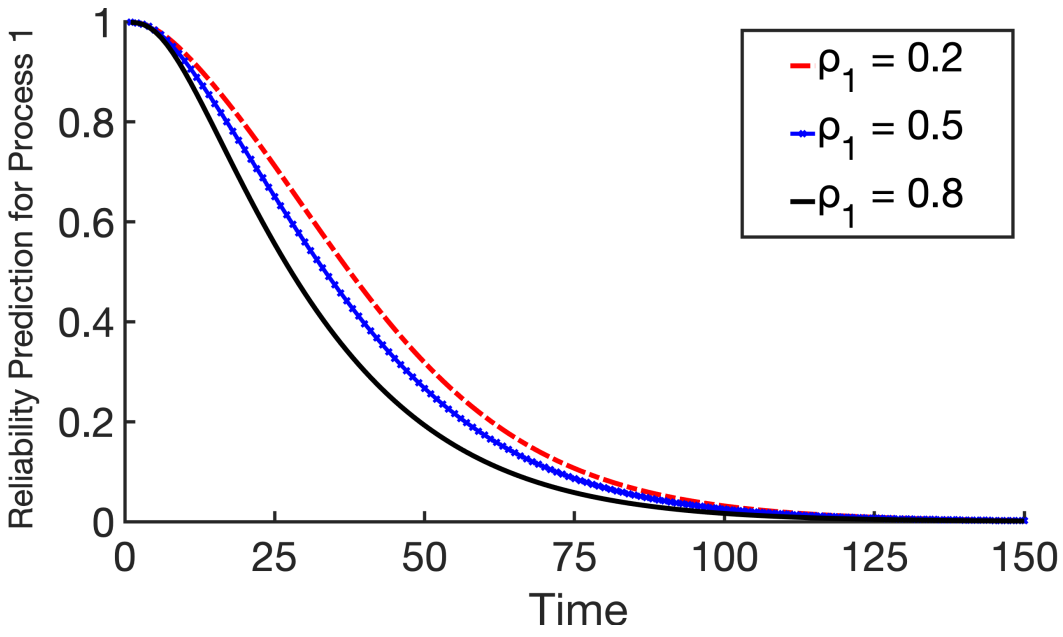

Fig. 6. Sensitivity analysis of process 1 with the changes of ρ_1.

In the degradation process 2, sensitivity analyses of ω_2, τ_2 and ρ_2 are conducted. The results are shown in Fig. 7, 8, and 9 respectively. According to Fig. 7, with a constant ω_2, the lifetime to failure at $\tau_2 = 1.2$ and $\tau_2 = 1.8$ is both approximately 100-time units. However, it significantly improves when $\tau_2 = 0.6$. From Fig. 8, degradation process 2 has a lifetime of roughly 125-time units when $\omega_2 = 0.3, 0.9, 1.5$. In Fig. 9, degradation process 2 has almost the same lifetime when $\rho_2 = 0.5$ and 0.8, while it increases a lot when $\rho_2 = 0.2$. Therefore, from these three figures, we can conclude that the sensitivity of ω_2 is not significant to the reliability prediction, while τ_2 and ρ_2 can influence the output more obviously.

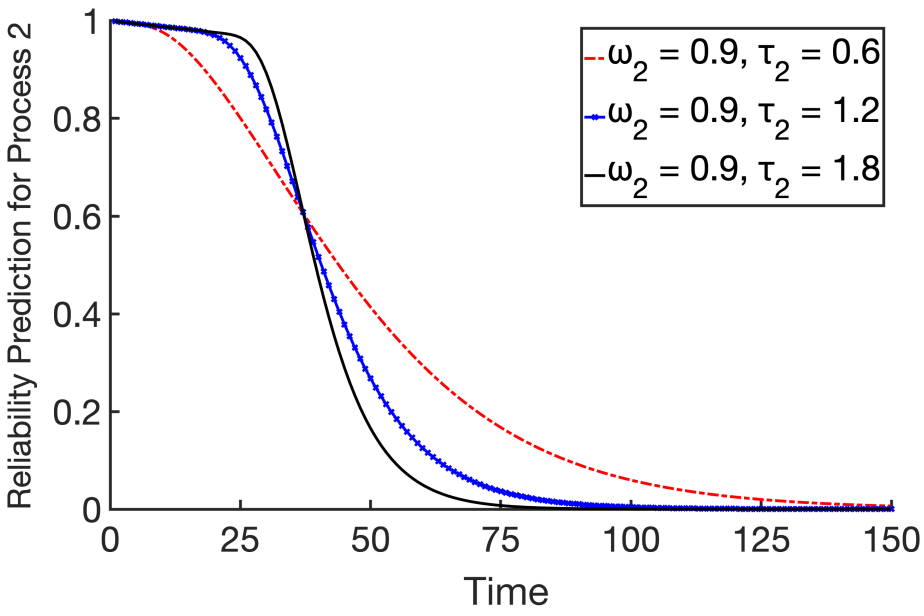

Fig. 7. Sensitivity analysis with the changes of τ_2.

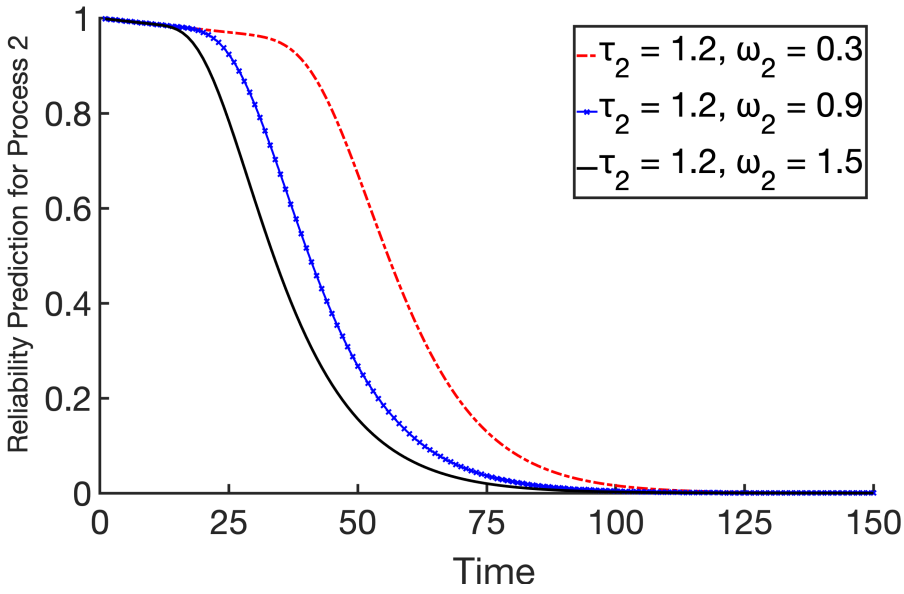

Fig. 8. Sensitivity analysis with the changes of ω_2.

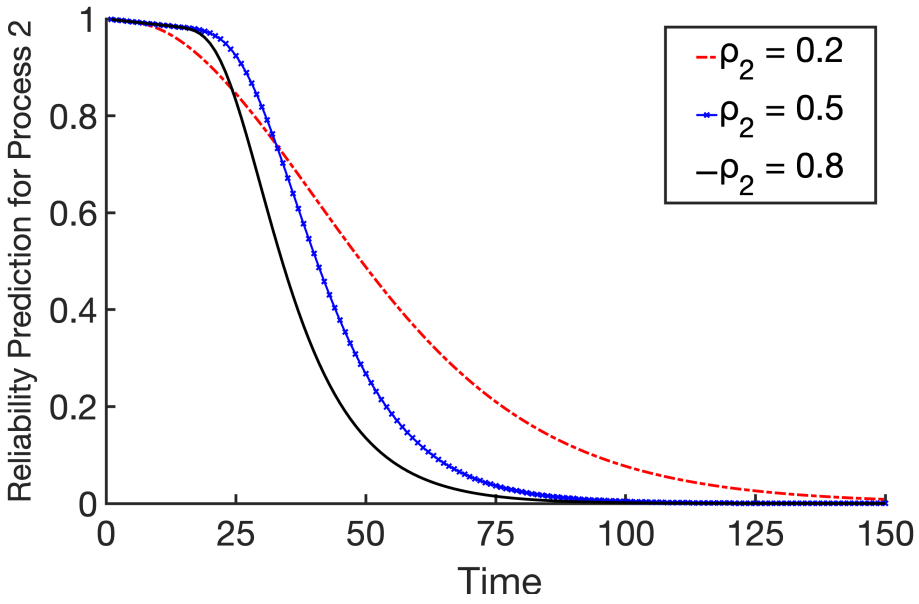

Fig. 9. Sensitivity analysis with the changes of ρ_2.

3.3.3 Copula Method

After getting marginal reliability functions, the copula method is applied to link them. Three Archimedean copulas including Frank, Clayton, Gumbel copulas, and their rotated copulas are implemented to fit the system reliability model. The goodness of fit is presented by using the criteria, log-likelihood, AIC, and BIC. The results are shown in Table II. Based on the definition of MLE, we aim to maximize the log-likelihood function since the larger log-likelihood is, the better copula fitting for these two degradations. Meanwhile, smaller AIC and BIC can also demonstrate better copula fitting. Comparing the result of log-likelihood in Table II, the value of Gumbel distribution is the largest, followed by Clayton copula. Rotated Clayton copula has the smallest log-likelihood. Therefore, we can conclude that the best copula fit among these six distributions is the Gumbel copula with log-likelihood as -1694.2, AIC as 3390.4, and BIC as 3393.5.

TABLE II
COMPARISONS OF THE GOODNESS OF FIT

Copulas	Parameter Estimation	Log-likelihood	AIC	BIC	Rank
Frank	17.1274	-1706.0	3414.0	3417.0	3
Clayton	0.7670	-1703.8	3409.5	3412.5	2
Gumbel	2.7255	-1694.2	3390.4	3393.5	1
Rotated Frank (180°)	11.8367	-1714.9	3431.7	3434.7	4
Rotated Clayton (180°)	1.1562	-1845.8	3693.6	3696.6	6
Rotated Gumbel (90°)	0.4851	-1733.4	3468.7	3471.8	5

3.3.4 System Reliability Estimation

Given the marginal reliability functions linked by copula distributions, the system reliability prediction is obtained by using Eq. (9). Fig. 10 shows the comparison of the joint distributions with six different copulas, which presents the result of the other five copulas except rotated Gumbel copula is close.

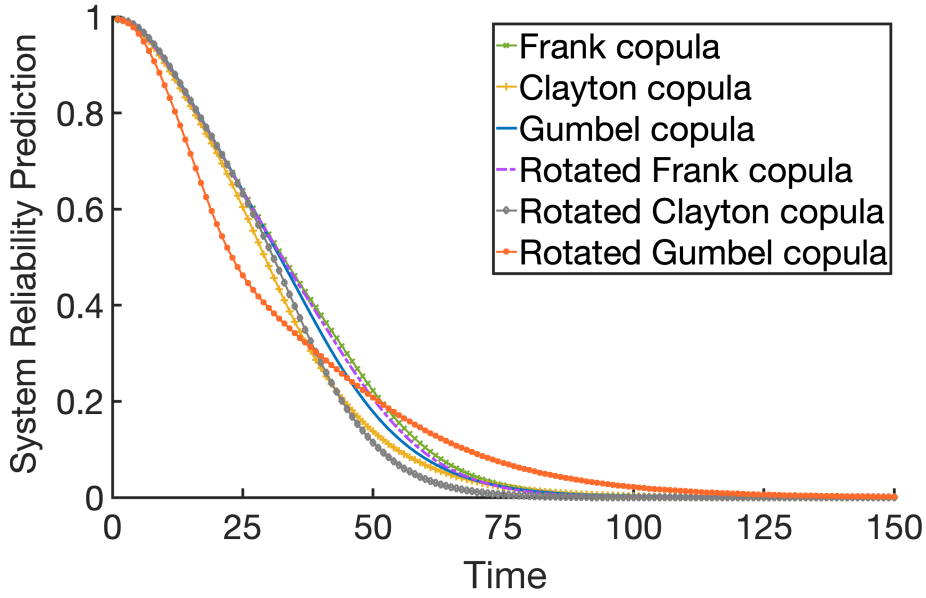

Fig. 10. Comparison of system reliability predictions with different copulas.

3.4 Numerical Example 2

3.4.1 System Description and Marginal Reliability Prediction

We apply the battery testing data collected from electric vehicles (EVs). Human behavior, such as charging time, charging type, and charging frequency influence HSA, which further affects battery degradation [44]. For example, Ning et al. [45] investigated that overcharge may increase battery's surface resistance, and then result in battery capacity degradation. Guo et al. [44] studied how charging habits influence battery degradation in EVs. They discovered that charge after use is more likely to cause damage to batteries than charge before use because of battery capacity loss.

In the battery management system, every single battery is regarded as a cell. Multiple cells are gathered as a module, a cluster of which are eventually installed as a pack. For one Li-ion battery charged to 4.2V, its battery pack can produce a total voltage of more than 400V for the EV [46]. Two Li-ion batteries testing data collected by B. Saha and K. Goebel [47] is applied to represent two degradation processes' performance: #25 battery was used in degradation process 1 and #26 battery in process 2. #25 battery is denoted as battery 1 and #26 battery for battery 2 in this thesis. In the experiment, battery 1 and battery 2 were run under three circumstances including charging, discharging, and impedance at 24 degrees Celsius. Charging was performed at 1.5A until the battery voltage reached 4.2V and then kept a constant voltage until the current reduced to 20mA. The discharge was performed using a 50% duty cycle until the battery voltage fell to 2.0V for battery 1 and 2.2V for battery 2. Impedance occurred under the frequency sweep from 0.1Hz to 5kHz. Every battery experienced discharge 28 times. Every time it was discharged, record the time consumed when the voltage dropped to its threshold (2.0V for battery 1, 2.2V for battery 2) for the first time. Table III and IV show the degradation data in batteries 1 and 2 individually. To obtain the degradation function for each battery, linear regressions were employed with two

variables: time consumed to 2V and the number of discharges. Since the sixth testing data for battery 2 is an outlier, it was not included. The degradation function for battery 1 is $y_1 = -2.11x_1 + 340$, where y_1 denotes the time that the voltage dropped to 2V in battery 1, x_1 denotes the number of discharges in process 1. The degradation function for battery 2 is $y_2 = -1.58x_2 + 325$, where y_2 denotes the time that the voltage dropped to 2V in battery 2, x_2 denotes the number of discharges in battery 2.

TABLE III
DEGRADATION DATA FOR BATTERY 1

X	1	2	3	4	5	6	7	8	9	10
Y	341	339	337	333	331	323	327	323	319	317
X	11	12	13	14	15	16	17	18	19	20
Y	315	313	311	309	307	305	299	297	301	299
X	21	22	23	24	25	26	27	28		
Y	297	295	293	291	289	287	285	281		

where x is the number of discharges, y is the time consumed when the voltage dropped to 2.0V.

TABLE IV
DEGRADATION DATA FOR BATTERY 2

X	1	2	3	4	5	6	7	8	9	10
Y	335	333	329	327	325	249	321	317	315	311
X	11	12	13	14	15	16	17	18	19	20
Y	297	309	307	305	303	301	281	293	299	297
X	21	22	23	24	25	26	27	28		
Y	295	291	291	289	287	285	283	281		

where x is the number of discharges, y is the time consumed when the voltage dropped to 2.2V.

Let the probability of nonfatal random shocks $q(t) = \exp(-\sigma t)$, where $\sigma = 0.002$. Let the rate of random shocks occurring $\lambda = 0.02$. In the battery 1 degradation process, given the probability of the LAL $\rho_1 = 0.5$. Y_1 follows an exponential distribution with CDF $F_Y(y) = 1 - \exp\left[-\frac{y}{\mu_1}\right]$, where $\mu_1 = 0.02$. The random shock loadings follow a normal distribution with

$N(1,4)$. HSA function $f(t)$ in the time-scaled factor is exponentially distributed with mean $\varepsilon_1 = 0.07$ and the coefficients in the time-scaled factor are ${\beta_1}^{(1)} = 0.05, {\beta_2}^{(1)} = 0.12, {\beta_3}^{(1)} = 0.03$. According to the degradation function for battery 1, the mean degradation wear of battery 1 is changed from $\varphi_1(t;\alpha_1)$ to $2.11\varphi_1(t;\alpha_1) + 340$. Let the failure threshold for process 1 is $l_1 = 70$. The marginal reliability prediction for battery 1 is shown in Fig. 11. In the battery 2 degradation process, assume that $\rho_2 = 0.5$and Y_2 follows an exponential distribution with parameter $\mu_2 = 0.05$. Assume the random shock loadings follow a normal distribution with $N(3, 0.64)$. $f(t)$ is the time-scaled factor follows an exponential distribution with mean $\varepsilon_2 = 0.08$ and coefficients in the time-scaled factor are ${\beta_1}^{(2)} = 0.06, {\beta_2}^{(2)} = 0.15, {\beta_3}^{(2)} = 0.05$. The mean degradation wear of battery 2 is changed from $\varphi_2(t;\alpha_2)$ to $1.58\varphi_1(t;\alpha_1) + 325$. Let the failure threshold for the battery 2 degradation process is $l_2 = 150$. Fig. 12 shows the marginal reliability prediction for battery 2.

As shown in Fig. 11 and 12, the lifetime to failure for battery 1 is roughly 80 and 60-time units for battery 2. Meanwhile, in the beginning, battery 1 can work in a significantly decent condition for a longer time compared with battery 2. Therefore, it seems the reliability of battery 1 is better than battery 2 according to the lifetime to failure and the duration under high efficiency working conditions.

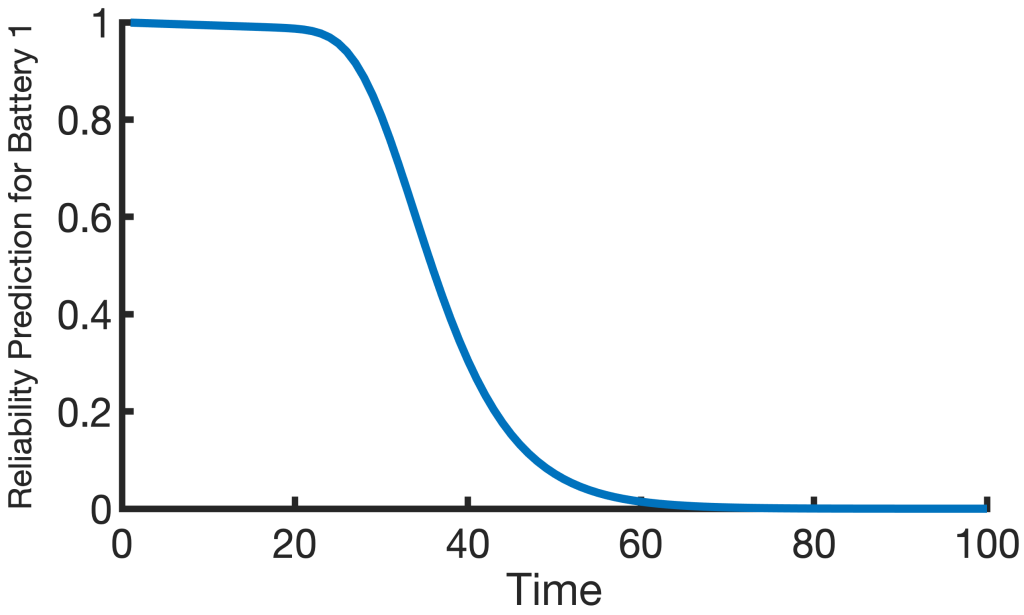

Fig. 11. Marginal reliability prediction for battery 1.

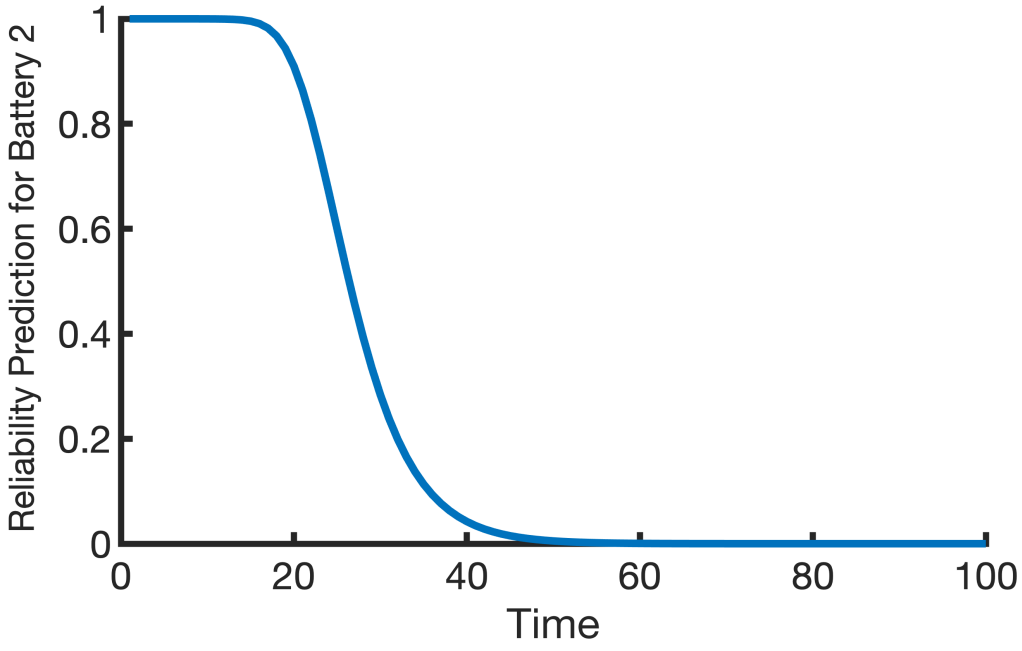

Fig. 12. Marginal reliability prediction for battery 2.

3.4.2 Sensitivity Analysis for Each Degradation Process

Sensitivity analyses are made for battery 1 and battery 2 to test how marginal reliability functions are influenced by parameters. In order to figure out how HSA affects battery degradation, we choose three parameters that are related to HSA to do the analyses: the mean of the exponential distribution, $f(t)$, denoted as ε_k, the probability of LAL ρ_k, and the coefficient of $f(t)$ in the time-scaled factor $F\left(t, \beta^{(k)}\right)$, denoted as ${\beta_3}^{(k)}$. Therefore, in the battery 1 degradation process, ε_1, ρ_1 and ${\beta_3}^{(1)}$ are applied and the results are shown in Fig. 13, 14, and 15. According to Fig. 13, the lifetime to the failure of battery 1 is roughly 80-time units when $\varepsilon_1 = 0.02$ and 0.07 and approximately 60-time units when $\varepsilon_1 = 0.12$. Hence, the lifetime has not much difference when ε_1 is changed from 0.02 to 0.07, however, it will decrease when ε_1 is changed to 0.12. From Fig. 14, battery 1 will fail faster with the increase of ${\beta_3}^{(1)}$, which indicates that HSA degradation can accelerate the battery's degradation rate. In Fig. 15, the lifetime to failure is almost the same on the condition that $\rho_1 = 0.2, 0.5$ and 0.8. So, the lifetime does not have much difference when ρ_1 changes but battery 1 starts to degrade in the early stage with ρ_1 increases.

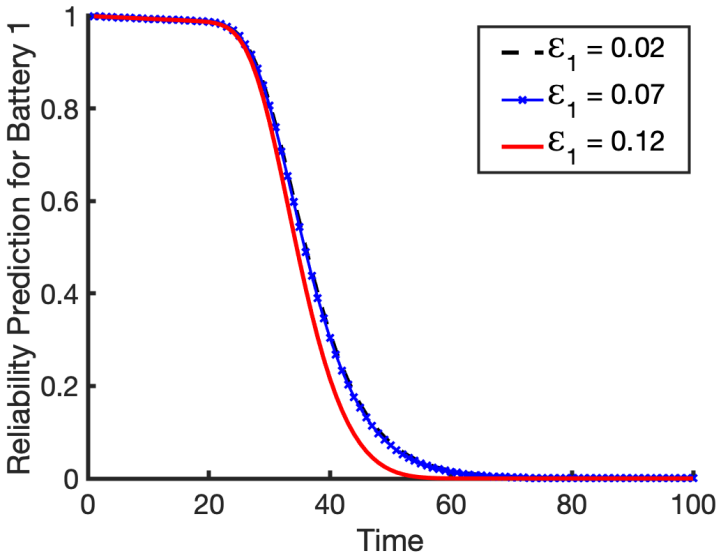

Fig. 13. Sensitivity analysis for battery 1 with the changes of ε_1.

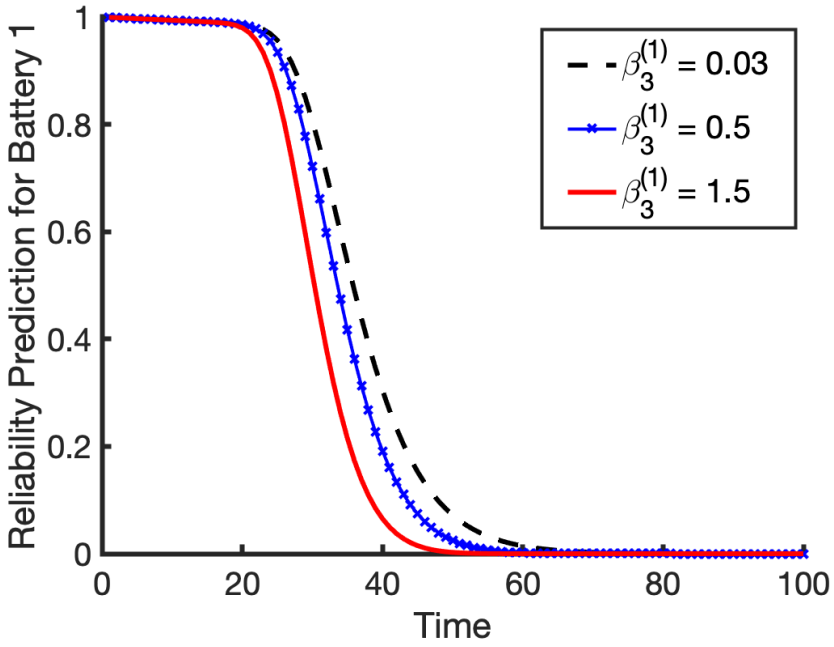

Fig. 14. Sensitivity analysis for battery 1 with the changes of $\beta_3{}^{(1)}$.

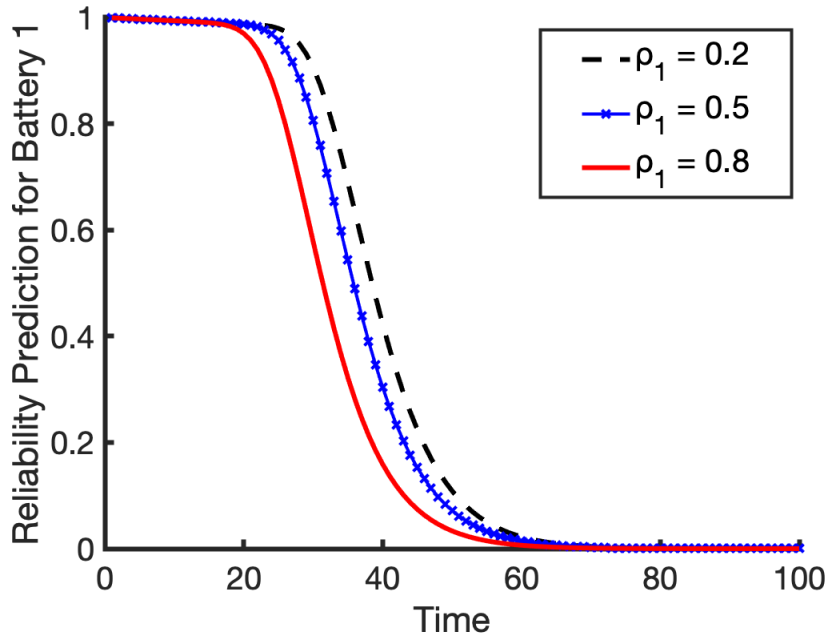

Fig. 15. Sensitivity analysis for battery 1 with the changes of ρ_1.

After doing sensitivity analysis for battery 1, the same tests were made for battery 2. Here, ε_2, ρ_2 and $\beta_3{}^{(2)}$ are utilized and the results are shown in Fig. 16, 17, and 18.

As illustrated in Fig. 16, the three lines are almost overlapped, which indicates that the sensitivity of ε_2 is not notable to the degradation process of battery 2. According to Fig. 17, when $\beta_3{}^{(2)} = 5$, the lifetime is shorter compared with the other situations, which indicates that HSA degradation contributes to the battery degradation acceleration. From Fig. 18, we can see that the change of ρ_2 does not influence the reliability prediction of battery 2 significantly.

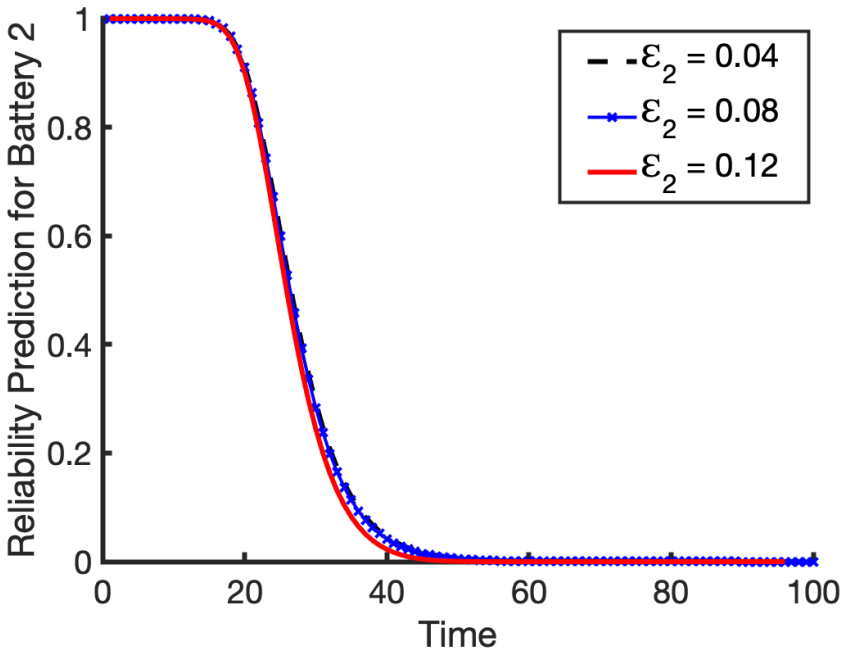

Fig. 16. Sensitivity analysis for battery 2 with the changes of ε_2.

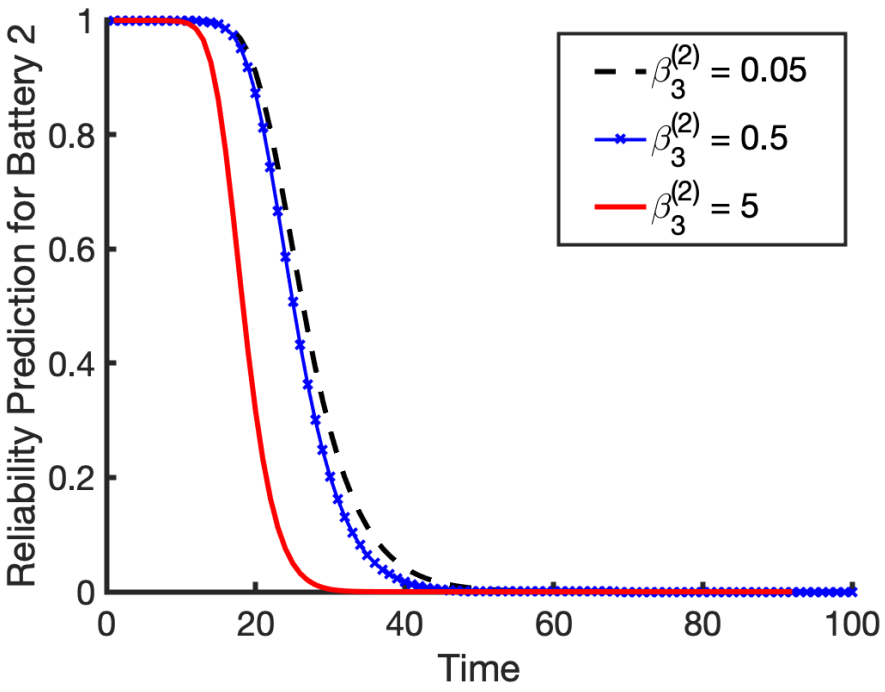

Fig. 17. Sensitivity analysis for battery 2 with the changes of ${\beta_3}^{(2)}$.

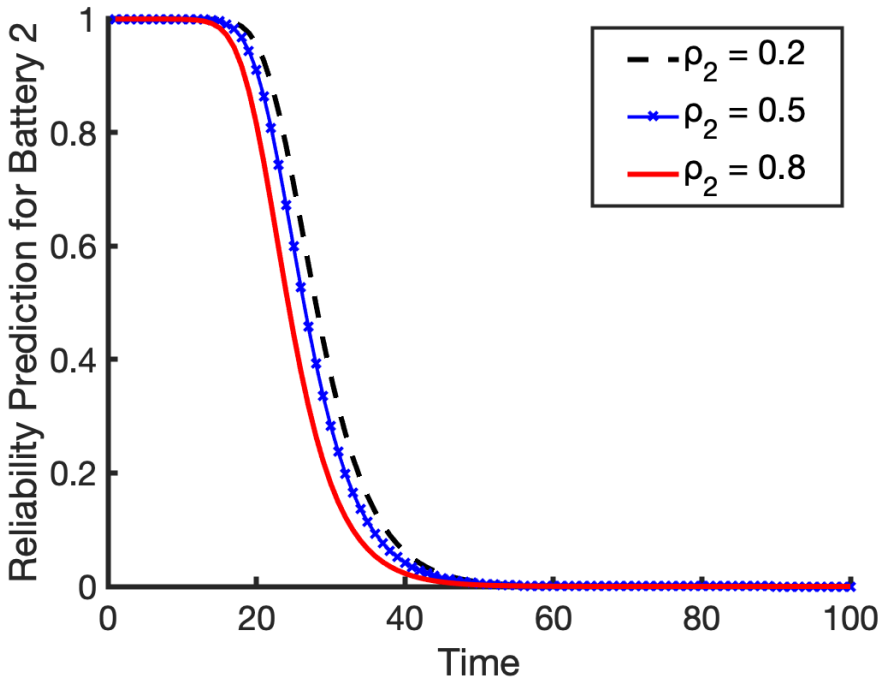

Fig. 18. Sensitivity analysis for battery 2 with the changes of ρ_2.

3.4.3 Copula Method

Three Archimedean copulas including Frank, Clayton, Gumbel copulas, and their rotated copulas are implemented to fit the system reliability model. Log-likelihood, AIC and BIC are served as criteria to the goodness of fit, as shown in Table V. From Table V, the Rotated Gumbel distribution is the most suitable copula distribution among these six distributions with log-likelihood as -1405.6, AIC as 2813.2, and BIC as 2815.8, followed by Clayton and Rotated Gumbel distribution. However, the rotated Clayton distribution is the worst copula with log-likelihood as -1610.3, AIC as 3222.7, and BIC as 3225.3.

TABLE V
COMPARISONS OF THE GOODNESS OF FIT

Copulas	Parameter Estimation	Log-likelihood	AIC	BIC	Rank
Frank	10.4594	-1570.5	3143.0	3145.6	4
Clayton	0.2837	-1449.8	2901.6	2904.2	3
Gumbel	2.1823	-1427.6	2857.1	2859.7	2
Rotated Frank (180°)	10.4593	-1570.5	3143.0	3145.6	4
Rotated Clayton (180°)	0.8449	-1610.3	3222.7	3225.3	6
Rotated Gumbel (90°)	0.4496	-1405.6	2813.2	2815.8	1

3.4.4 System Reliability Prediction

After getting the joint copula functions, the system reliability function is derived by using Eq. (11). Fig. 19 shows the comparison of joint reliability functions with different copulas. From Fig. 19, we can see that the reliability prediction model with a rotated Gumbel copula is much higher than others.

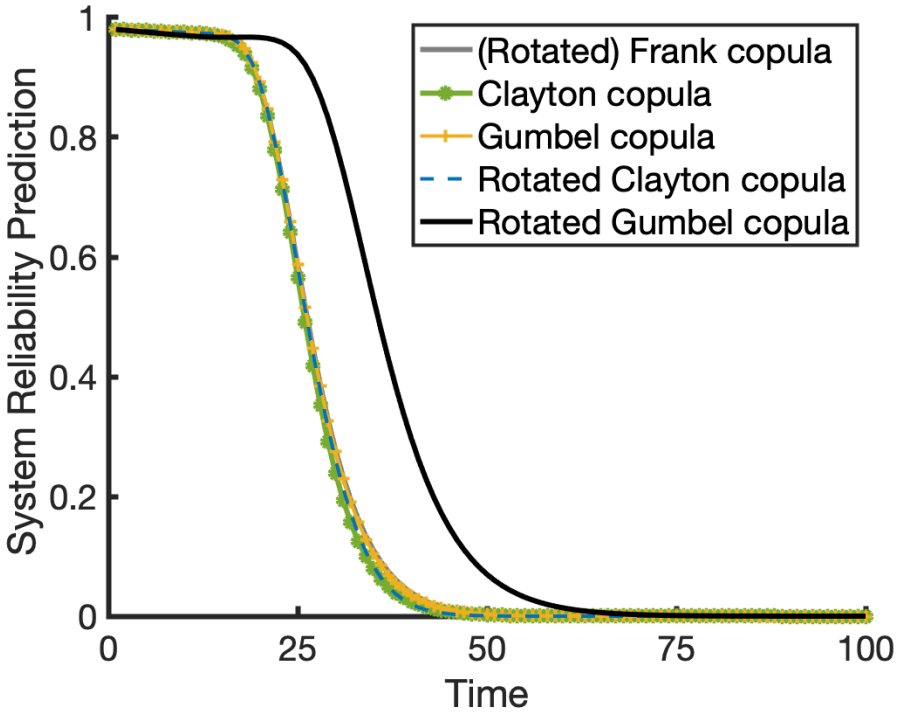

Fig. 19. Comparison of system reliability predictions with different copulas.

CHAPTER 4: CONCLUSION

This study established an HMI system reliability model, which not only considers the impacts of HSA on the health state of the machine but multiple degradation processes and random shocks. The copula method is used to solve the dependency between multiple degradation processes. HMI system reliability estimation is finalized by multiplying the joint copula function with the probability of nonfatal random shocks. The copula parameters are estimated by using MLE. Log-likelihood, AIC and BIC are served as criteria to check the goodness of copula fit. Besides the model comparison criteria, selection methods from a mathematical perspective are also briefly discussed. In the two numerical examples, sensitivity analysis for different parameters is made to check how they influence system reliability. For future research, due to HSA incorporated in this thesis, it is interesting to think about a method to minimize the impact of HSA on machine degradation and develop a maintenance policy given on this issue.

REFERENCES

[1] A. Elasyed, “Reliability and Hazard Functions,” in *Reliability Engineering*, 2nd ed., 2012.

[2] L. Justin, “10 Biggest Car and Truck Recalls Since 2000,” Oct. 2019, Available online: https://www.motorbiscuit.com/10-biggest-car-and-truck-recalls-since-2000/.

[3] P. Wang, and D. W. Coit, “Reliability prediction based on degradation modeling for systems with multiple degradation measures,” in *Annual Symposium Reliability and Maintainability*, Los Angeles, CA, USA, Jan. 2004, pp. 302-307.

[4] Y. Wang, and H. Pham, "Modeling the dependent competing risks with multiple degradation processes and random shock using time-varying copulas," *IEEE Trans. Rel.*, vol. 61, no. 1, pp. 13-22, Mar. 2012.

[5] V. Crk, “Reliability assessment from degradation data,” in *Annual Reliability and Maintainability Symposium, 2000 Proceedings, International Symposium on Product Quality and Integrity*, Los Angeles, CA, USA, Jan. 2000, pp. 155-161.

[6] M. Zhu, “A new framework of complex system reliability with imperfect maintenance policy,” *Annals of Operations Research*. DOI: https://doi.org/10.1007/s10479-020-03852-w.

[7] Z. Pan, N. Balakrishnan, Q. Sun, and J. Zhou, “Bivariate degradation analysis of products based on wiener processes and copulas,” *Journal of Statistical Computation and Simulation*, vol. 83, no. 7, pp. 1316-29, Jul. 2013.

[8] M. Zhu, and H. Pham, “A novel system reliability modeling of hardware, software, and interactions of hardware and software,” Mathematics, 7(11), 1049, Nov. 2019.

[9] M. Fan, Z. Zeng, E. Zio, and R. Kang, “Modeling dependent competing failure processes with degradation-shock dependence,” *Reliability Engineering & System Safety*, vol. 165, pp. 422-430, Sep. 2017.

[10] J. D. Esary, and A. W. Marshall, “Shock models and wear processes,” *Annals of Probability*, vol. 1, no. 4, pp. 627-649, Aug. 1973.

[11] S. Eryilmaz, and C. Kan, “Reliability and optimal replacement policy for an extreme shock model with a change point,” *Reliability Engineering and System Safety*, vol. 190, p. 106513, Oct. 2019.

[12] F. Mallor, and J. Santos, “Classification of shock models in system reliability,” *Monografias del Semin. Matem. Garcıa de Galdeano*, vol. 27, pp. 405-412, 2003.

[13] W. Li, and H. Pham, “An inspection-maintenance model for systems with multiple competing processes,” *IEEE Transactions on Reliability*, vol. 54, no. 2, pp. 318-27, May. 2005.

[14] Y. H. Lin, Y. F. Li, and E. Zio, “Reliability assessment of systems subject to dependent degradation processes and random shocks,” *IIE Transactions*, vol. 48, no. 11, pp. 1072-1085, Jun. 2016.

[15] Z. Wang, H. Huang, Y. Li, and N. Xiao, "An approach to reliability assessment under degradation and shock process," *IEEE Trans. Rel.*, vol. 60, no. 4, pp. 852-863, Dec. 2011.

[16] K. Rafiee, Q. Feng, and D.W. Coit, “Reliability modeling for dependent competing failure processes with changing degradation rate,” *IIE Transactions*, vol. 46, no. 5, pp. 483-96, Feb. 2014.

[17] M. Corbett, "From law to folklore: work stress and the Yerkes-Dodson Law," *Journal of Managerial Psychology*, vol. 30, no. 6, pp. 741-752, Aug. 2015.

[18] S. H. Seo, S. H. Kwak, S. C. Chung, H. S. Kim, and B. C. Min, “Effect of distraction task on driving performance of experienced taxi drivers,” *Asian Biomedicine*, vol. 11, no. 4, pp. 315-322, Mar. 2018.

[19] J. Fan, and A. P. Smith, "The impact of workload and fatigue on performance," in *International Symposium on Human Mental Workload: Models and Applications, Springer, Cham*, vol. 726, Jun. 2017, pp. 90-105.

[20] N. I. Abd Rahman., S. Z. M. Dawal, and N. Yusoff, "Driving mental workload and performance of aging drivers," *Transportation Research Part F: Traffic Psychology and Behaviour*, vol. 69, pp. 265-285, Feb. 2020.

[21] M. R. Endsley, and D. J. Garland, "Theoretical underpinnings of situation awareness: a critical review", *Situation Awareness Analysis and Measurement*, vol. 1, no.1, pp. 3-21, 2000.

[22] M. R. Endsley, "Toward a theory of situation awareness in dynamic systems", *Human Factors*, vol. 37, no.1, pp. 32-64, Mar. 1995.

[23] Z. Liu, X. Ma, J. Yang, and Y. Zhao, "Reliability modeling for systems with multiple degradation processes using inverse Gaussian process and copulas," *Mathematical Problems in Engineering*, vol. 2014, pp. 1 - 10, Jun. 2014.

[24] J. Kolesár, P. Koščák, V. Begera, and Z. Šusterová, "The role and the Place of human in the system of human–machine," in Aeronautika 17, s 86-94, Lublin: University College of Enterprise and Administration, Jan. 2017.

[25] M. Havlikova, M. Jirgl, and Z. Bradac, "Human reliability in man-machine systems," *Procedia Engineering*, vol. 100, pp. 1207-1214, 2015.

[26] M. A. B. Alvarenga, P. F. Melo, and R. A. Fonseca, "A critical review of methods and models for evaluating organizational factors in Human Reliability Analysis," *Progress in Nuclear Energy*, vol. 75, pp. 25-41, Aug. 2014.

[27] J. C. de Winter, Y. B. Eisma, C. Cabrall, P. A. Hancock, and N. A. Stanton, "Situation awareness based on eye movements in relation to the task environment," *Cognition, Technology & Work*, vol. 21, no. 1, pp. 99-111, Feb. 2019.

[28] Z. M. Becerra, "Measuring the Influence of Automation on Situation Awareness in Highly Automated Vehicles," Doctoral dissertation, School of Phycology, Georgia Institute of Technology, Atlanta, GA, Apr. 2020.

[29] M. Jipp and P. L. Ackerman, "The impact of higher levels of automation on performance and situation awareness: a function of information-processing ability and working-memory capacity," *Journal of Cognitive Engineering and Decision Making*, vol. 10, no. 2, pp. 138-166, Mar. 2016.

[30] A. G. Smith, and G. A. Jamieson, "Level of automation effects on situation awareness and functional specificity in automation reliance," in *Proceedings of the Human Factors and Ergonomics Society Annual Meeting*, Los Angeles, CA, USA, Sep. 2012, pp. 2113-2117.

[31] B. Bashiri and D. D. Mann, "Automation and the situation awareness of drivers in agricultural semi-autonomous vehicles," *Biosystems Engineering*, vol. 124, pp. 8-15, Aug. 2014.

[32] R. Pasupathy, "Generating homogeneous Poisson processes," *Wiley Encyclopedia of Operations Research and Management Science*, June 2010.

[33] S. J. Bae, W. Kuo, and P. H. Kvam, "Degradation models and implied lifetime distributions," *Reliability Engineering & System Safety*, vol. 92, no.5, pp. 601-608, May 2007.

[34] M. Kyriakidis, J. C. de Winter, N. Stanton, T. Bellet, B. van Arem, K. Brookhuis, M. H. Martens, K. Bengler, J. Andersson, and N. Merat, "A human factors perspective on automated driving," *Theoretical Issues in Ergonomics Science*, vol. 20, no. 3, pp. 223-249, May 2019.

[35] N. Kolev, U. d. Anjos, and Mendes, Beatriz Vaz de M, "Copulas: A review and recent developments," *Stochastic Models*, vol. 22, no.4, pp. 617-660, Apr. 2006.

[36] A. I. Requena, L.Mediero, and L. Garrote, "Bivariate return period based on copulas for hydrologic dam design: comparison of theoretical and empirical approach," *Hydrology & Earth System Sciences Discussions*, vol. 10, no. 1, Jan. 2013.

[37] A. Wiboonpongse, J. Liu, S. Sriboonchitta, and T. Denoeux, "Modeling dependence between error components of the stochastic frontier model using copula: application to intercrop coffee production in Northern Thailand," *International Journal of Approximate Reasoning*, vol. 65, pp. 34-44, Oct. 2015.

[38] S. M. Lo, and R. A. Wilke, "A copula model for dependent competing risks," *Journal of the Royal Statistical Society: Series C (Applied Statistics)*, vol. 59, no. 2, pp. 359-376, Feb. 2015.

[39] B. K. Beare, "Copulas and temporal dependence," *Econometrica*, vol. 78, no. 1, pp. 395-410, Feb. 2010.

[40] M. D. Ward and J. S. Ahlquist, "Maximum Likelihood for Social Science: Strategies for Analysis," *Cambridge University Press*, New York, USA, Nov. 2018.

[41] H. d. Acquah, "Comparison of Akaike information criterion (AIC) and Bayesian information criterion (BIC) in selection of an asymmetric price relationship," *Journal of Development and Agricultural Economics*, vol. 2, no. 1, pp. 001-006, Jan. 2010.

[42] C. Giraud, *Introduction to high-dimensional statistics*, Boca Raton, FL, USA, Dec. 2014.

[43] A. Saltelli, M. Ratto, T. Andres, F. Campolongo, J. Cariboni, D. Gatelli, M. Saisana, S. Tarantola, Iooss, Bertrand, and Andrea Saltelli, "Introduction to sensitivity analysis," Handbook of uncertainty quantification, Dec. 2017, pp. 1103-1122.

[44] J. Guo, J. Yang, W. Cao, and C. Serrano, “Evaluation of EV battery degradation under different charging strategies and V2G schemes,” RPG, Shanghai, China, Oct. 2019, pp. 264-7.

[45] G. Ning, B. Haran, and B. N. Popov, “Capacity fade study of lithium-ion batteries cycled at high discharge rates,” *Journal of Power Sources*, vol. 117, no. 1-2, pp. 160-169, May 2003.

[46] Nissan Motor Corporation, “Electric vehicle lithium-ion battery,” Available online: https://www.nissan-global.com/e n/technology/overview/l i_ion_ev.html.

[47] B. Saha and K. Goebel, "Battery data set", NASA Ames Prognostics Data Repository, NASA Ames Research Center, Moffett Field, CA, 2007, Available online: http://ti.arc.nasa.gov/project/prognostic-data-repository.